

PAPER

[View Article Online](#)
[View Journal](#)

Cite this: DOI: 10.1039/d0cy01864c

Zirconium and hafnium polyhedral oligosilsesquioxane complexes – green homogeneous catalysts in the formation of bio-derived ethers *via* a MPV/etherification reaction cascade†

Shipra Garg, , Daniel K. Unruh and Clemens Krempner *

The polyhedral oligosilsesquioxane complexes, $\{[(\text{isobutyl})_7\text{Si}_7\text{O}_{12}]\text{ZrOPr}^i(\text{HOPr}^i)}_2$ (I), $\{[(\text{cyclohexyl})_7\text{Si}_7\text{O}_{12}]\text{ZrOPr}^i(\text{HOPr}^i)}_2$ (II), $\{[(\text{isobutyl})_7\text{Si}_7\text{O}_{12}]\text{HfOPr}^i(\text{HOPr}^i)}_2$ (III) and $\{[(\text{cyclohexyl})_7\text{Si}_7\text{O}_{12}]\text{HfOPr}^i(\text{HOPr}^i)}_2$ (IV), were synthesized in good yields from the reactions of $\text{M(OPr}^i)_4$ ($\text{M} = \text{Zr, Hf}$) with R-POSS(OH)_3 ($\text{R} = \text{isobutyl, cyclohexyl}$), resp. I–IV were characterized by ^1H , ^{13}C and ^{29}Si NMR spectroscopy and their dimeric solid-state structures were confirmed by X-ray analysis. I–IV catalyze the reductive etherification of 2-hydroxy- and 4-hydroxy and 2-methoxy and 4-methoxybenzaldehyde and vanillin to their respective isopropyl ethers in isopropanol as a “green” solvent and reagent. I–IV are durable and robust homogeneous catalysts operating at temperatures of 100–160 °C for days without significant loss of catalytic activity. Likewise, I–IV selectively catalyze the conversion of 5-hydroxymethylfurfural (HMF) into 2,5-bis(isopropoxymethyl)furan (BPMF), a potentially high-performance fuel additive. Similar results were achieved by using a combination of $\text{M(OPr}^i)_4$ and ligand R-POSS(OH)_3 as a catalyst system demonstrating the potential of this “*in situ*” approach for applications in biomass transformations. A tentative reaction mechanism for the reductive etherification of aldehydes catalysed by I–IV is proposed.

Received 22nd September 2020,
Accepted 23rd October 2020

DOI: 10.1039/d0cy01864c

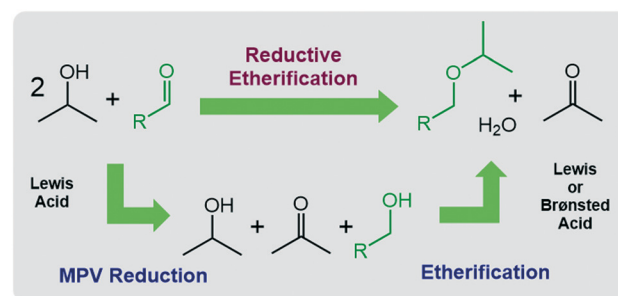
rsc.li/catalysis

Introduction

The chemical conversion of cellulosic biomass into liquid fuel, is a subject of current interest from both the industrial as well as the academic perspective.¹ Particularly, alkyl ethers have become intensively investigated in the last few years owing to their potential application as high-performance fuel additives.² One of the most promising synthetic strategies for alkyl ethers involves the reductive etherification of biomass-derived aldehydes *via* the Meerwein–Ponndorf–Verley (MPV) reaction followed by acid-catalysed etherification (Scheme 1).³

This process is operationally simple and environmentally friendly as it utilizes “green” isopropanol as an inexpensive, safe and non-toxic solvent and hydrogen transfer reagent in combination with cheap and abundant acid catalysts. The MPV reduction,⁴ the first step in the cascade, proceeds *via* Lewis acid-catalysed hydrogen transfer usually from a

secondary alcohol to the carbonyl substrate with high selectivity, following an outer-sphere mechanism,⁵ while the etherification proceeds with elimination of water and can be catalysed by both, Brønsted or Lewis acid catalysts. Indeed, some heterogeneous tin, zirconium and hafnium zeolite and oxide based catalysts have been reported to convert 5-hydroxymethylfurfural (HMF), a platform chemical for biofuels, biochemical and biopolymers,⁶ into 2,5-bis(isopropoxy-methyl)furan (BPMF)⁷ *via* reductive etherification. In contrast, homogeneous catalysts capable of



Scheme 1 Ether formation from aldehydes *via* a reductive etherification cascade.

Department of Chemistry and Biochemistry, Texas Tech University, Memorial Dr. & Boston, Lubbock, TX, 79409, USA. E-mail: clemens.krempner@ttu.edu;

Fax: +806 742 1289; Tel: +806 834 3507

† Electronic supplementary information (ESI) available. CCDC 2009174–2009177. For ESI and crystallographic data in CIF or other electronic format see DOI: 10.1039/d0cy01864c

converting HMF into BPMF with high selectivity and yields have not yet been reported.⁸

Early transition metal “polyhedral” oligosilsesquioxane (POSS) complexes⁹ of a tripodal coordination geometry are a largely overlooked class of robust and durable metal complexes that have shown some potential as homogeneous catalysts in alkene epoxidations¹⁰ and polymerizations.¹¹ The electron-withdrawing properties of the POSS ligand combined with its steric profile give rise to well-defined metal complexes that possess relatively high Lewis acidity while maintaining good chemical resistance. Herein, we will introduce zirconium and hafnium POSS complexes as a new class of highly efficient and remarkably thermally-stable homogeneous catalysts for selected biomass transformations as demonstrated for the reductive etherification of HMF to biofuel additive, BPMF.

Results and discussion

The synthesis of the targeted zirconium and hafnium POSS complexes **I–IV** is illustrated in Scheme 2. Reaction of the commercially available trisilanols R-POSS(OH)₃ (R = isobutyl or cyclohexyl) with Zr(OPrⁱ)₄ and Hf(OPrⁱ)₄, respectively, gave, after removal of solvent and precipitation or recrystallization from isopropanol (IPA), compounds **I–IV** in 58–66% yield. **I–IV** are thermally stable crystalline materials, which show good solubility in toluene, hexanes, benzene, dichloromethane, diethyl ether and THF but are sparingly soluble in alcohols and DMSO. In addition to be characterized by ¹H, ¹³C and ²⁹Si NMR spectroscopy and combustion analysis, the solid-state structures of **I–IV** were determined by X-ray analysis. The results are shown for **I** and **III** (Fig. 1); selected bond lengths and angles for **I–IV** are listed in Table 1.

In the solid state, all compounds are isostructural dimers with distorted octahedral coordination environments for zirconium and hafnium, respectively. The coordination sphere of each metal centre is completed by coordinated isopropanol, similar to what is seen for other titanium and zirconium analogues.¹² The dimers are held together *via* bridging isopropoxide groups and hydrogen bond interaction between the OH group of the coordinated isopropanol and an oxygen from one of the metal binding siloxy groups [O1⋯O7H, 2.99 to 3.12 Å]. There are three

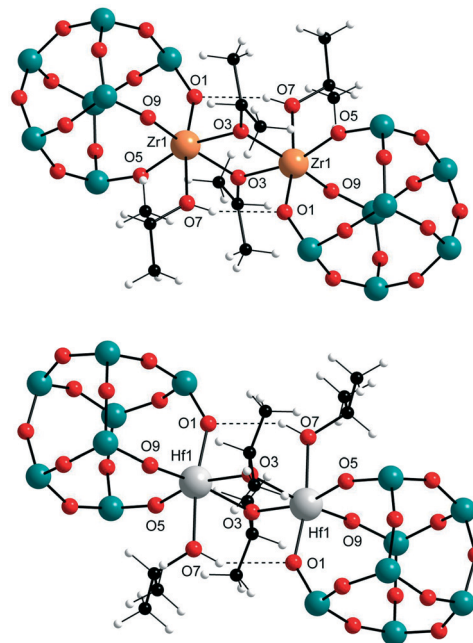
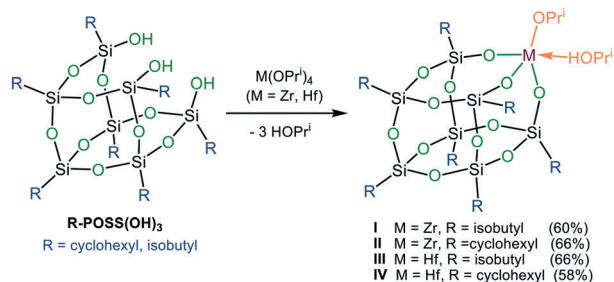


Fig. 1 Solid-state structures of **I** (top) and **III** (bottom); isobutyl substituents at the silicon atoms are omitted for clarity (blue = silicon, red = oxygen).

types of metal–oxygen bonds that result from this structural arrangement: bridging M–O bonds [M1–O3, 2.14–2.18 Å], M–O bonds of the coordinated isopropanol [M1–O7, 2.26–2.30 Å], and M–O bonds from the supporting POSS ligand [M1–O1/O5/O9, 1.97–2.02 Å]. As expected, the M1–O7 distances are significantly longer than the bridging M1–O3 and POSS related M–O distances, suggesting a relatively weak isopropanol to metal coordination.

With the POSS complexes **I–IV** in hand, we investigated their catalytic performance in the reductive etherification of various benzaldehydes along with their precursors Zr(OPrⁱ)₄ and Hf(OPrⁱ)₄. Initial screening experiments at 25–70 °C did not show any substrate conversion. Therefore, the experiments were carried out in closed reaction vessels at temperatures ranging from 100 °C to 150 °C with a catalyst loading of 1 mol%. Isopropanol (IPA) served as solvent and hydrogen transfer reagent and was used as received (“wet”). Conversions and product yields were determined by ¹H NMR



Scheme 2 Synthesis of **I–IV**.

Table 1 Selected bond lengths [Å] and angles [°] of **I–IV**

| | I (M = Zr) | II (M = Zr) | III (M = Hf) | IV (M = Hf) |
|-----------------------|-------------------|--------------------|---------------------|--------------------|
| M1–O1 | 2.015(3) | 1.997(1) | 1.993(5) | 1.995(2) |
| M1–O3 | 2.177(3) | 2.156(1) | 2.136(5) | 2.146(2) |
| M1–O5 | 1.982(3) | 1.988(1) | 1.967(5) | 1.984(2) |
| M1–O7 | 2.304(3) | 2.303(2) | 2.257(5) | 2.274(2) |
| M1–O9 | 1.966(3) | 1.987(1) | 1.973(5) | 1.982(2) |
| O1–M1–O7 | 164.8(1) | 170.4(1) | 167.9(2) | 170.3(1) |
| Si–O(M1) ^a | 1.611(3) | 1.612(2) | 1.606(5) | 1.612(2) |

^a Average values.

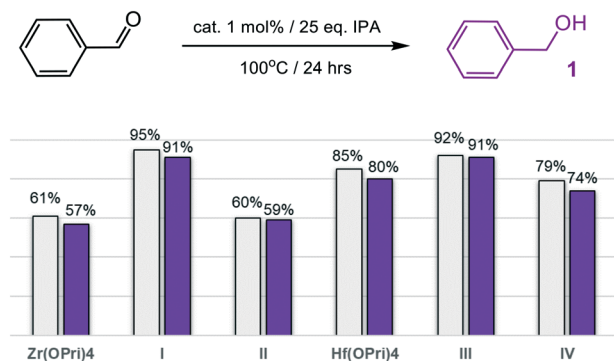


Fig. 2 MPV reduction of benzaldehyde to benzyl alcohol (1): conversions (grey bars) and yields of alcohol 1 (purple bars).

spectroscopy using CDCl_3 as a solvent and 1,3,5-trimethylbenzene as internal standard. The catalytic experiments were triplicated and conversions and product yields were given as average values.

The moisture sensitive precursors $\text{Zr}(\text{OPri})_4$ and $\text{Hf}(\text{OPri})_4$ were found to be surprisingly active in selectively reducing benzaldehyde to benzyl alcohol (1) in “wet” isopropanol (IPA) with yields of 57% and 80%, respectively, after 24 hours at 100 °C (Fig. 2). The employment of the new POSS complexes I–IV reproducibly allowed for higher yields with catalysts I and III each producing 91% of 1. At 150 °C, no differences in the performance were noted between I–IV, $\text{Zr}(\text{OPri})_4$ and $\text{Hf}(\text{OPri})_4$; all quantitatively reduced benzaldehyde to 1 (Table S1†), but did not form benzyl isopropyl ether.

Next, the reduction of the more electron-rich 4-methoxybenzaldehyde was investigated (Fig. 3). Similar to what was seen in the previous case, all zirconium and hafnium based catalysts reduced 4-methoxybenzaldehyde to 4-methoxybenzyl alcohol (2) in good to excellent yields after 24 hours at 100 °C. $\text{Hf}(\text{OPri})_4$ and I showed the best catalyst performances generating 94% of alcohol 2, respectively.

Notably, increasing the temperatures from 100 to 150 °C not only improved conversions but also changed the selectivity markedly in favour of the targeted 4-methoxybenzyl

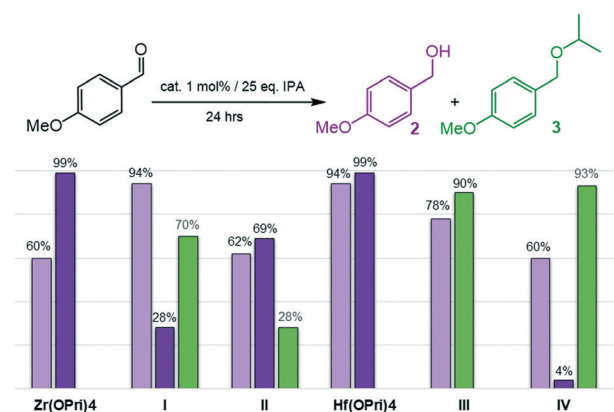


Fig. 3 Reductive etherification of 4-methoxybenzaldehyde: yields of alcohol 2 at 100 °C (light purple bars); yields of alcohol 2 (dark purple bars) and ether 3 (green bars) at 150 °C.

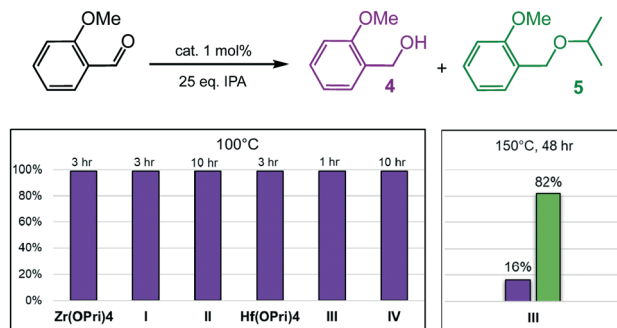


Fig. 4 Reductive etherification of 2-methoxybenzaldehyde: (left graph) yields of alcohol 4 (purple bars) at various times; (right graph) yields of alcohol 4 (purple bar) and ether 5 (green bar) after 48 hours.

isopropyl ether (3). While $\text{Hf}(\text{OPri})_4$ and $\text{Zr}(\text{OPri})_4$ quantitatively converted 4-methoxybenzaldehyde into alcohol 2 only, the hafnium complexes III and IV selectively produced ether 3 in yields of 90% and 93%, respectively.

2-Methoxybenzaldehyde was converted much faster and with better selectivity into its respective alcohol at 100 °C than 4-methoxybenzaldehyde regardless of the catalyst used (Fig. 4 and Tables S3 and S4†). In fact, isobutyl substituted POSS complex I, $\text{Zr}(\text{OPri})_4$ and $\text{Hf}(\text{OPri})_4$ quantitatively generated 2-methoxybenzyl alcohol (4) in only 3 hours at 100 °C. The cyclohexyl substituted complexes II and IV were slightly less active presumably due to their poor solubility in IPA at 100 °C. However, complex III proved to be the most active and selective catalyst. III not only quantitatively produced alcohol 4 in 1 hour, it also converted alcohol 4 into ether 5 upon increasing the temperature to 150 °C. In fact, III generated, after 24 hours, 57% of 5 along with 39% of alcohol 4. After 48 hours, 82% of 5 and 16% of 4 were formed (Fig. 4).

Given the structural similarities of I–IV (*vide supra*), it remains unclear why only III generates significant amounts of ether 5. It is known that chelating substrates often cause metal-catalyzed reactions to be sluggish because of the inherent strength of the resulting product–metal bonds,

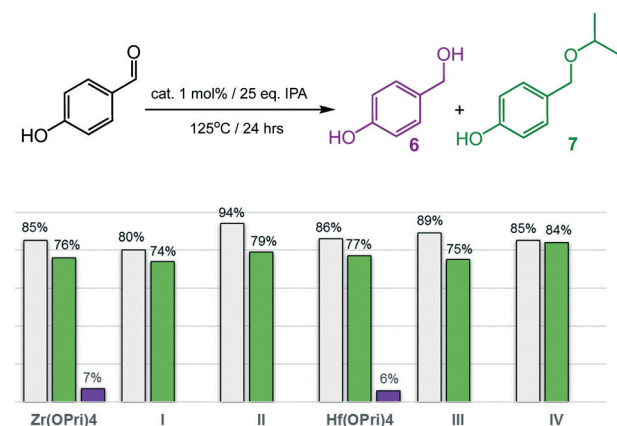


Fig. 5 Reductive etherification of 4-hydroxybenzaldehyde. Conversions (grey bars): yields of alcohol 6 (purple bars); yields of ether 7 (green bars).

typically the limiting factor in product liberation from the metal catalyst. Therefore, even the subtle changes of the steric profile (isobutyl *versus* cyclohexyl substituents) and the identity of the metal (zirconium or hafnium) may account for the differences in product selectivity.

Encouraged by the ability to selectively catalyse the formation of ethers, the more challenging substrates 2-hydroxy- and 4-hydroxybenzaldehyde were investigated (Fig. 5 and 6). To our surprise, complexes **I–IV** smoothly catalysed the formation of the corresponding isopropyl ethers **7** and **9**, respectively, which were obtained in good to excellent yields after 24 hours. 2-Hydroxybenzaldehyde was found to convert into **9** faster and at slightly lower temperatures (120 °C) than 4-hydroxybenzaldehyde, which required 125 °C to be converted into ether **7** in acceptable yields. Notably, also the precursors $\text{Zr}(\text{OPri})_4$ and $\text{Hf}(\text{OPri})_4$ catalysed the formation of ethers **7** and **9**, respectively, from their respective aldehydes with similar yields but somewhat lower selectivity.

Having had success in selectively producing hydroxy ethers **7** and **9**, vanillin (4-hydroxy-3-methoxybenzaldehyde), one of the most widely used aroma chemicals and fragrances that can be produced from biomass-derived lignin, was examined (Fig. 7). Astonishingly, all zirconium and hafnium catalysts converted vanillin into isopropyl ether **10** with high selectivity and in yields ranging from 68–91%, even though higher temperatures (150 °C) were required relative to the reductive etherification of 2- and 4-hydroxybenzaldehyde. Of all the catalysts used, **IV** proved to be the most active system as 91% of ether **10** were formed after 24 hours at 150 °C. The catalyst performance of **IV** is similar to that of Rode's dual heterogeneous catalyst, which is composed of $\text{ZrO}(\text{OH})_2$ and Zr-montmorillonite, and gave **10** in 80% yield after 8 hours at 100 °C.^{7c}

Unfortunately, efforts to reduce the phenolic aldehydes 3,4-dihydroxybenzaldehyde and 4-hydroxy-3,5-methoxybenzaldehyde (syringe aldehyde) failed. After 2 days at 150 °C, no conversion was noted. We attribute the inability of these multi-functionalized aldehydes to undergo reduction

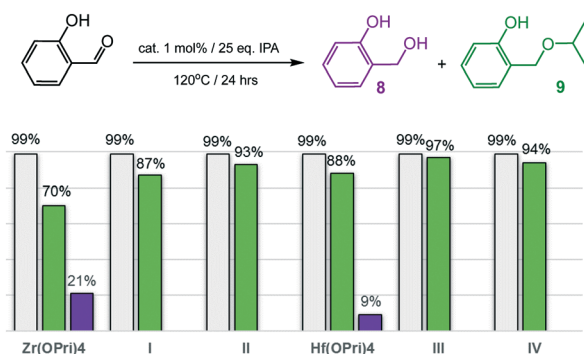


Fig. 6 Reductive etherification of 4-hydroxybenzaldehyde. Conversions (grey bars): yields of alcohol **8** (purple bars); yields of ether **9** (green bars).

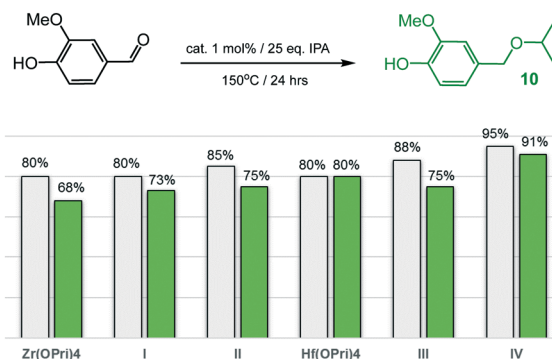


Fig. 7 Reductive etherification of vanillin: conversions (grey bars) and yields of ether **10** (green bars).

to their metal chelating properties, resulting in deactivation of the catalyst.

In comparing the results described above, we noticed that $\text{Zr}(\text{OPri})_4$ and $\text{Hf}(\text{OPri})_4$ were fairly active in catalysing the formation of hydroxy ethers **7**, **9** and **10**, but did not catalyse the formation of methoxy ethers **3** and **5**. Moreover, 2- and 4-hydroxybenzaldehyde were converted faster and with better selectivity to the corresponding ethers than 2- and 4-methoxybenzaldehyde regardless of the catalyst used. At first glance, this appeared to be counter intuitive as according to the Hammett sigma constants, OH groups are somewhat stronger electron donors than methoxy groups. This results in lower carbonyl activities for 2- and 4-hydroxybenzaldehyde, and consequently would lead to lower rates of reduction.

To gain more insights, the kinetic profiles of the reductive etherification for all the five benzaldehydes were obtained at 100 °C with 1 mol% of **III** as the catalyst; the results are shown in Fig. 8 and 9. Consistent with our expectation based

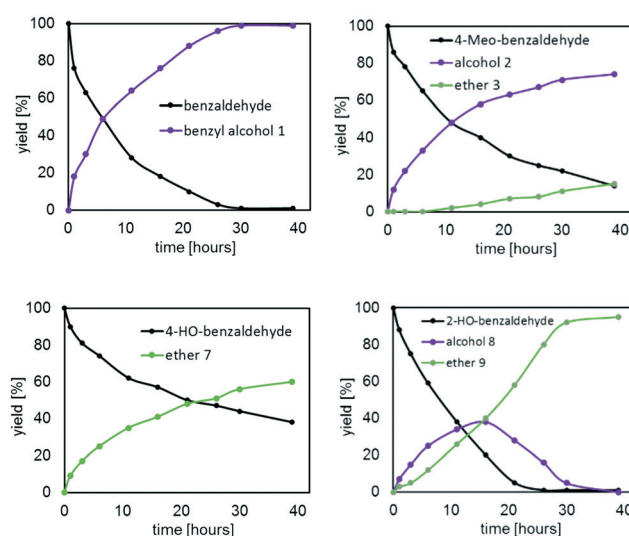


Fig. 8 Kinetic profiles of the reductive etherification of benzaldehyde, 4-MeO-benzaldehyde, 4-HO-benzaldehyde and 2-HO-benzaldehyde. Reaction conditions: 100 °C, cat. **III** (1 mol%), 25 eq. isopropanol (IPA).

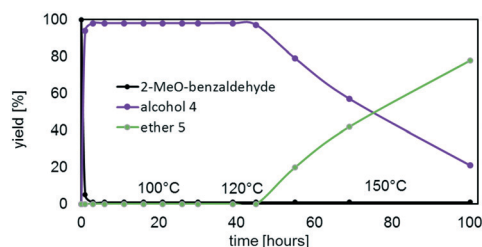


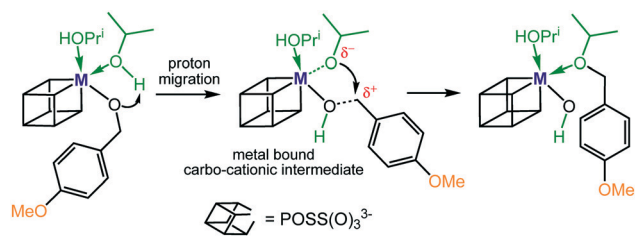
Fig. 9 Kinetic profile of the reductive etherification of 2-MeO-benzaldehyde as a function of temperature. Reaction conditions: 100 °C (0–39 hours), 120 °C (39–45 hours), 150 °C (45–99 hours); cat. **III** (1 mol%), 25 eq. isopropanol (IPA).

on the Hammett constants, the rate of conversion was found to be in the order $\text{C}_6\text{H}_5\text{CHO}$ (82%; 16 hours) > 4-MeO- $\text{C}_6\text{H}_4\text{-CHO}$ (60%; 16 hours) > 4-HO- $\text{C}_6\text{H}_4\text{CHO}$ (43%; 16 hours).

The catalytic behaviour of **III** in the reductive etherification of 2-methoxybenzaldehyde (Fig. 9) warrants an additional comment. After having catalysed the quantitative formation of alcohol **4** in less than an hour, and being further heated at 100 °C for 39 hours and at 120 °C for additional 6 hours, **III** still preserves its catalytic activity. In fact, upon subsequently increasing the temperature to 150 °C, alcohol **4** slowly converts into ether **5**, demonstrating the catalysts' long-term durability and robustness at high temperatures over extensive periods of time and in the presence of water.

We noticed that benzaldehyde and 2-methoxybenzaldehyde exclusively converted into their respective alcohols, and only 4-methoxybenzaldehyde produced small quantities of ether after 30 hours at 100 °C. Therefore, it is reasonable to assume that the slow step of the reductive etherification for these substrates is the metal-catalysed alcohol etherification. Ether formation most likely proceeds *via* a metal stabilized intermediate of carbo-cationic character generated from proton migration of one of the coordinating IPA molecules (Scheme 3). Additional stabilization arises from the electron-donating 4-MeO group, enabling an intramolecular nucleophilic attack of isopropoxide to form the ether bond.

The active involvement of carbo-cationic intermediates is supported by the observation that at 150 °C the methoxy alcohols **2** and **4** convert to the respective ethers but not benzyl alcohol **1**, *i.e.* the cationic benzyl intermediate is markedly less stable than the 2- and 4-methoxy substituted

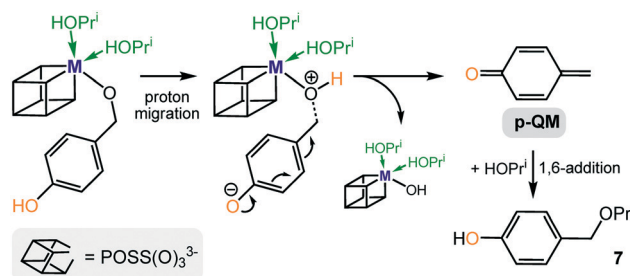


Scheme 3 Proposed ether formation *via* a metal bound carbo-cationic intermediate.

counterparts. One of the key factors that enables rapid and selective ether formation seems to be the Lewis acidity of the catalyst system. This is supported by the observation that **I–IV** catalyse the etherification of methoxy alcohols **2** and **4** but not $\text{Zr}(\text{OPr}^i)_4$ and $\text{Hf}(\text{OPr}^i)_4$, *i.e.* **I–IV** are stronger Lewis acids than their precursors because of the stronger electron-withdrawing properties of the POSS ligand *versus* an aliphatic alkoxide ligand.¹³

By contrast, the precursors $\text{Zr}(\text{OPr}^i)_4$ and $\text{Hf}(\text{OPr}^i)_4$ not only catalyse the reductive etherification of 2- and 4-hydroxybenzaldehyde and vanillin (Fig. 5–7), their activity is surprisingly similar to those of **I–IV**. In addition, the kinetic results for catalyst **III** (Fig. 8 and 9) further confirm that 2- and 4-hydroxybenzaldehyde were converted much faster into their respective ethers than 2- and 4-methoxybenzaldehyde. It seems that these drastic differences in rates are not accounted for by the slightly better ability of the 2- and 4-hydroxy groups to stabilize the carbo-cationic intermediate than the 2- and 4-methoxy groups (Scheme 3). Therefore, we propose an alternative mechanism that involves the formation of *ortho*- or *para*-quinone methide intermediates,¹⁴ which are formed *via* proton migration of the phenolic proton followed by cleavage of the benzylic C–O bond (Scheme 4). These reactive Michael acceptors, which have been generated from various organic precursors and used extensively in synthetic organic chemistry,¹⁵ can be described as benzylic cations that are strongly stabilized by the resonance electron-donating 4-O[–] or 2-O[–] substituents.¹⁶ As a result, they are more stable than the cationic methoxybenzyl intermediates involved in the formation of methoxy ethers **3** and **5**, nonetheless, can readily be attacked by the external nucleophile isopropanol (present in excess) to form the corresponding hydroxy ethers **7**, **9** and **10**, respectively.

We next investigated the reduction of HMF, an important renewable feedstock for various bio-based organic compounds such as 2,5-bis(hydroxymethyl)furan (BHMF) (**11**), furan-dicarboxylic acid, levulinic acid, ethyl levulinate and derivatives thereof. Employing Sn-Beta as the catalyst, Vlachos and co-worker reported the formation of BPMF (**12**) from HMF with 87% selectivity and up to 80% overall yield at 180 °C.^{7b} Rode *et al.* disclosed the conversion of HMF into



Scheme 4 Proposed alternative formation of hydroxy ether **7** *via* a metal stabilized *para*-quinone methide intermediate (*p*-QM = *para*-quinone methide).

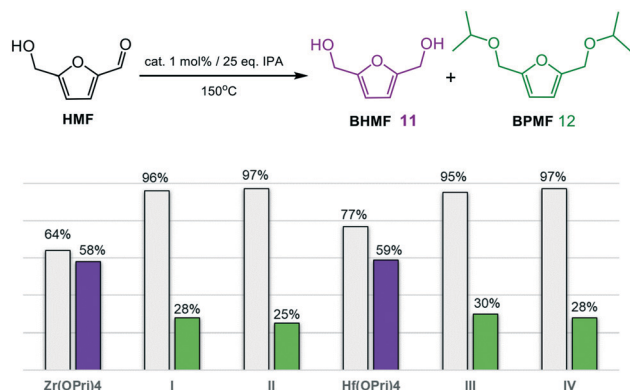


Fig. 10 Reductive etherification of 2-hydroxymethylfurfural (HMF). Conversions (grey bars) and product yields (purple bars = **11**; green bars = **12**) after 4 hours.

BPMF (**12**) in isopropanol at 150 °C with claimed selectivity of up to 95% using the dual catalysts, ZrO(OH)₂ and Zr-montmorillonite.^{7c} However, in neither cases have isolated yields been reported.

As the reductive etherification of HMF is a complex chemical transformation that involves the formation of humin polymers¹⁷ and various other synthetic intermediates,^{7c} we were pleased to see that the simple precursors Zr(OPr)₄ and Hf(OPr)₄ selectively generated BHMF (**11**) in good yields of 58% and 59%, resp., in only 4 hours at 150 °C (Fig. 10).

In contrast, catalysts **I–IV** quantitatively converted HMF into primarily humin polymers and the desired BPMF (**12**),

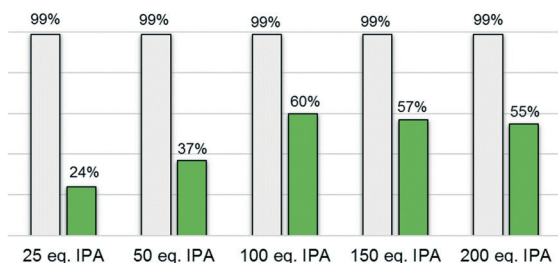
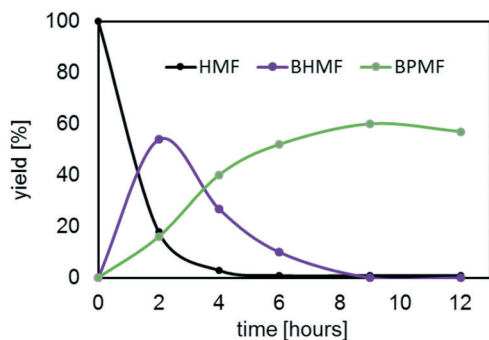


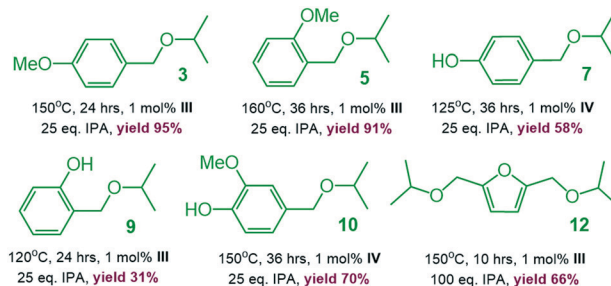
Fig. 11 Reductive etherification of HMF as a function of isopropanol (IPA) eq.; cond.: 9 hours, 150 °C, cat. **III** (1 mol%); top: kinetic profile for 100 eq. of IPA; bottom: conversions (grey bars) and yields of BPMF **12** (green bars) for various eq. of IPA.

albeit the latter in fairly low yields (25–30%). Increasing the reaction time proved to be counter-productive as the yields of **12** further decreased in favour of humin polymers, a common problem in this chemistry.¹⁷ To suppress the formation of humin polymers, a series of experiments was undertaken, where the HMF concentration was gradually decreased by increasing the amounts of isopropanol, from 25 up to 200 eq. using **III** as the catalyst at 150 °C. The most relevant results are summarized in Fig. 11 (see also Fig. S17–S21†) and revealed the optimum conditions for this process to be *ca.* 9–10 hours and 100 eq. of isopropanol. Gratifyingly, after 9 hours, both HMF and undesired BHMF (**11**) were fully consumed, and the reaction mixture only contained *ca.* 60% BPMF (**12**) and polymer, which greatly facilitated the purification process. Again, increasing the reaction time led to a slight decrease in the yields of **12** due to polymer formation.

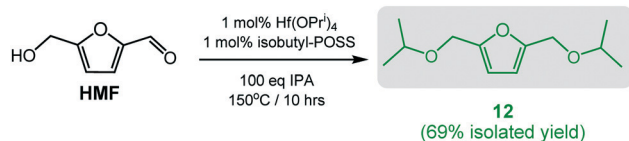
To demonstrate the practicality of our homogeneous catalyst approach, scale-up syntheses of ethers **3**, **5**, **7**, **9**, **10** and **12** (1 g substrate) were carried out employing the best performing catalysts, resp. (Scheme 5). All products except **7** could easily be purified by vacuum distillation with isolated yields ranging from to 31–94% (ref. 18) without the need of tedious purification by column chromatography.

The efficacy and robustness of catalyst **III** in the conversion of HMF to BPMF (**12**), prompted us to test the catalytic activity of Hf(OPr)₄ (1 mol%) in the presence of ligand Buⁱ-POSS(OH)₃ (Scheme 6). Gratifyingly, after *ca.* 10 hours at 150 °C (100 eq. IPA) and subsequent purification by vacuum distillation, BPMF could be isolated in 69% yield, similar to what was observed with isolated **III** as the catalyst. Since Hf(OPr)₄ itself does not produce BPMF (*vide supra*), catalyst **III** appears to have formed during the course of the reaction. This “*in situ*” catalyst approach could also be applied to the catalytic formation of ethers **3**, **5** and **10** with comparable isolated yields but somewhat longer reaction times (see ESI†).

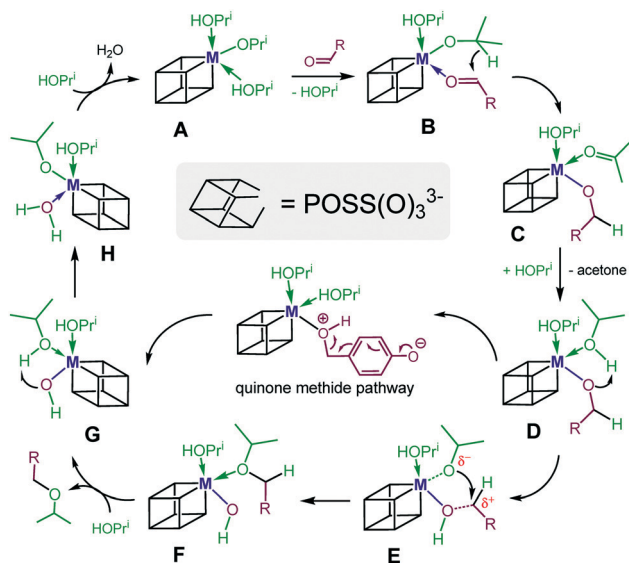
To study the catalyst structure in the solution, diffusion experiments for hafnium complex **III** using DOSY-NMR spectroscopy were performed in various solvents at room temperature. The results for THF-D₈ and C₆D₆ suggest **III** to be dimeric in solution, which is consistent with its solid-state structure. In the more polar solvents CD₂Cl₂ and acetone-D₆,



Scheme 5 Gram scale synthesis of **3**, **5**, **7**, **9**, **10** and **12**.



Scheme 6 Synthesis of **10** and **12** employing 1 mol% Hf(OPr)_4 and 1 mol% $\text{Bu}^i\text{-POSS(OH)}_3$.



Scheme 7 Proposed reaction mechanism of the reductive etherification of aldehydes.

however, **III** was found to be monomeric (for more details see ESI†).

Based on these observations and those discussed above, we propose a tentative mechanism, where **III** exists in isopropanol as a hexa-coordinate monomeric complex of type **A** (Scheme 7). For the MPV reduction to occur, complex **A**, which bears two coordinated IPA molecules, needs to be in rapid equilibrium with its substrate-metal complex **B** to allow for an intramolecular transfer of hydride from the isopropoxide to the substrate. Complex **C** thus generated then converts *via* replacement of the coordinated acetone product with excess IPA into species **D**. To enable the second step of the overall process, the etherification, an intramolecular proton transfer in **D** from the coordinated IPA to the benzyloxide, needs to occur. Complex **E** thus generated then undergoes an intramolecular nucleophilic substitution to furnish the ether bound metal hydroxide **F**. Liberation of the coordinated ether product from **F** *via* replacement with excess IPA produces metal hydroxide **G**. Subsequent intramolecular proton transfer from the coordinated IPA to the hydroxide generates complex **H**. The latter finally converts to catalyst **A** upon replacement of the coordinated water molecule by excess IPA. Note that in the case of 2- and 4-hydroxybenzaldehyde and vanillin as substrates, proton migration in species **D** will occur involving the phenolic proton. This is followed by C–O bond cleavage and formation of *ortho*- or *para*-quinone methide intermediates (see also Scheme 4).

Conclusions

With the goal of developing durable homogeneous catalysts for selective biomass transformations, we have synthesized tripodal zirconium and hafnium isopropoxides **I–IV**. In these “corner capped” complexes, zirconium and hafnium are rigidly incorporated into the electron-withdrawing POSS(O)_3^{3-} ligand framework, which provides complexes **I–IV** with sufficient Lewis acidity, high kinetic stability and thermal robustness. In fact, **I–IV** are efficient homogeneous catalysts operating at low loadings and high temperatures in the reductive etherification of electron-rich aromatic aldehydes to produce various isopropyl ethers. Zr(OPr)_4 and Hf(OPr)_4 are active catalysts themselves, showing excellent selectivity toward the formation of alcohols **2**, **4** and **11** but are inactive regarding ether formation. These selectivity differences can be interpreted in terms of their different Lewis acidities. In contrast, **I–IV** and $\text{Zr(OPr)}_4/\text{Hf(OPr)}_4$ generated the hydroxyl ethers **7**, **9** and **10** with similar activities and selectivities, which we attribute to the involvement of *para*- and *ortho*-quinone methide intermediates. Most importantly, **III** proved to be the first homogeneous catalyst capable of selectively converting HMF into bio-fuel additive BPMF (**12**), the latter could be isolated in good yields and purities upon distillation. That similar catalytic performances can be achieved without the need of synthesizing the POSS catalyst, as demonstrated for the selective conversion of HMF into BPMF, highlights the potential of our homogeneous approach for applications in biomass and related transformations.

Conflicts of interest

There are no conflicts to declare.

Acknowledgements

This research was supported by the U.S. Department of Energy, Office of Science, Office of Basic Energy Sciences, Catalysis Science Program, under Award DE-SC0019094. We are grateful to Anthony Cozzolino for calculating the van der Waals volume of complex **III** and Shiva Moaven for assisting in the DOSY-NMR experiments.

Notes and references

- (a) M. J. Climent, A. Corma and S. Iborra, *Green Chem.*, 2014, **16**, 516–547; (b) J. C. Serrano-Ruiz and J. A. Dumesic, *Energy Environ. Sci.*, 2011, **4**, 83–99; (c) D. M. Alonso, J. Q. Bond and J. A. Dumesic, *Green Chem.*, 2010, **12**, 1493–1513.
- (a) A. Liu, B. Liu, Y. Wang, R. Ren and Z. Zhang, *Fuel*, 2014, **117**, 68–73; (b) M. Balakrishnan, E. R. Sacia and A. T. Bell, *Green Chem.*, 2012, **14**, 1626–1634; (c) M. Musolino, M. J. Gines-Molina, R. Moreno-Tost and F. Arico, *ACS Sustainable Chem. Eng.*, 2019, **7**, 10221–10226.
- (a) A. Corma and M. Renz, *Angew. Chem., Int. Ed.*, 2007, **46**, 298–300; (b) A. M. Rasero-Almansa, M. Iglesias and F.

- Sanchez, *RSC Adv.*, 2016, **6**, 106790–106797; (c) G. Li, L. Gao, Z. Sheng, Y. Zhan, C. Zhang, J. Ju, Y. Zhang and Y. Tang, *Catal. Sci. Technol.*, 2019, **9**, 4055–4065.
- 4 (a) C. Battilocchio, J. M. Hawkins and S. V. Ley, *Org. Lett.*, 2013, **15**, 2278–2281; (b) B. McNerney, B. Whittlesey, D. B. Cordes and C. Krempner, *Chem. – Eur. J.*, 2014, **20**, 14959–14964; (c) X. Wang, J. Hao, L. Deng, H. Zhao, Q. Liu, N. Li, R. He, K. Zhi and H. Zhou, *RSC Adv.*, 2020, **10**, 6944–6952; (d) A. Corma, M. E. Domine, L. Nemeth and S. Valencia, *J. Am. Chem. Soc.*, 2002, **124**, 3194–3195; (e) K. Flack, K. Kitagawa, P. Pollet, C. A. Eckert, K. Richman, J. Stringer, W. Dubay and C. L. Liotta, *Org. Process Res. Dev.*, 2012, **16**, 1301–1306.
 - 5 (a) R. Cohen, C. R. Graves, S. T. Nguyen, J. M. L. Martin and M. A. Ratner, *J. Am. Chem. Soc.*, 2004, **126**, 14796–14803; (b) O. Eisenstein and R. H. Crabtree, *New J. Chem.*, 2013, **37**, 21–27; (c) R. S. Assary, L. A. Curtiss and J. A. Dumesic, *ACS Catal.*, 2013, **3**, 2694–2704.
 - 6 (a) R.-J. van Putten, J. C. van der Waal, E. de Jong, C. B. Rasrendra, H. J. Heeres and J. G. de Vries, *Chem. Rev.*, 2013, **113**, 1499–1597; (b) S. Chen, R. Wojcieszak, F. Dumeignil, E. Marceau and S. Royer, *Chem. Rev.*, 2018, **118**, 11023–11117.
 - 7 (a) J. Luo, J. Yu, R. J. Gorte, E. Mahmoud, D. G. Vlachos and M. A. Smith, *Catal. Sci. Technol.*, 2014, **4**, 3074–3081; (b) J. Jae, E. Mahmoud, R. F. Lobo and D. G. Vlachos, *ChemCatChem*, 2014, **6**, 508–513; (c) S. Shinde and C. Rode, *ChemSusChem*, 2017, **10**, 4090–4101.
 - 8 H. Nguyen, N. Xiao, S. Daniels, N. Marcella, J. Timoshenko, A. Frenkel and D. G. Vlachos, *ACS Catal.*, 2017, **7**, 7363–7370.
 - 9 (a) F. J. Feher and T. A. Budzichowski, *Polyhedron*, 1995, **14**, 3239–3253; (b) D. B. Cordes, P. D. Lickiss and F. Rataboul, *Chem. Rev.*, 2010, **110**, 2081–2173; (c) C. Krempner, *Eur. J. Inorg. Chem.*, 2011, **2011**, 1689–1698.
 - 10 (a) H. C. L. Abbenhuis, S. Krijnen and R. A. van Santen, *Chem. Commun.*, 1997, 331–332; (b) T. Maschmeyer, M. C. Klunduk, C. M. Martin, D. S. Shephard, J. M. Thomas and B. F. G. Johnson, *Chem. Commun.*, 1997, 1847–1848; (c) M. Crocker, R. H. M. Herold and A. G. Orpen, *Chem. Commun.*, 1997, 2411–2412; (d) F. Carniato, C. Bisio, E. Boccaleri, M. Guidotti, E. Gavrilova and L. Marchese, *Chem. – Eur. J.*, 2008, **14**, 8098–8101; (e) E. H. Aish, M. Crocker and F. T. Ladipo, *J. Catal.*, 2010, **273**, 66–72; (f) M. D. Skowronska-Ptasinska, M. L.-W. Vorstenbosch, R. A. van Santen and H. C. L. Abbenhuis, *Angew. Chem., Int. Ed.*, 2002, **41**, 637–639; (g) L. Zhang, H. C. L. Abbenhuis, G. Gerritsen, N. N. Bhriain, P. C. M. Magusin, B. Mezari, W. Han, R. A. van Santen, Q. Yang and C. Li, *Chem. – Eur. J.*, 2007, **13**, 1210–1221; (h) P. Guillo, M. I. Lipschutz, M. E. Fasulo and T. D. Tilley, *ACS Catal.*, 2017, **7**, 2303–2312.
 - 11 (a) F. J. Feher, J. F. Walzer and R. L. Blanski, *J. Am. Chem. Soc.*, 1991, **113**, 3618–3619; (b) F. J. Feher and R. L. Blanski, *J. Am. Chem. Soc.*, 1992, **114**, 5886–5887; (c) R. Duchateau, H. C. L. Abbenhuis, R. A. van Santen, A. Meetsma, S. K.-H. Thiele and M. F. H. van Tol, *Organometallics*, 1998, **17**, 5663–5673.
 - 12 (a) O. Viotti, A. Fischer, G. A. Seisenbaeva and V. G. Kessler, *Inorg. Chem. Commun.*, 2010, **13**, 774–777; (b) O. Viotti, G. A. Seisenbaeva and V. G. Kessler, *Inorg. Chem.*, 2009, **48**, 9063–9065.
 - 13 (a) F. J. Feher and T. A. Budzichowski, *J. Organomet. Chem.*, 1989, **379**, 33–40; (b) R. West and R. H. Baney, *J. Am. Chem. Soc.*, 1959, **81**, 6145–6148; (c) R. West, R. H. Baney and D. L. Powell, *J. Am. Chem. Soc.*, 1960, **82**, 6269–6272; (d) P. T. Wolczanski, *Polyhedron*, 1995, **14**, 3335–3362; (e) C. Krempner, *Eur. J. Inorg. Chem.*, 2011, 1689–1698.
 - 14 (a) *Quinone Methides*, ed. S. E. Rokita, John Wiley and Sons, 2009; (b) E. Dorrestijn, M. Kranenburg, M. V. Ciriano and P. Mulder, *J. Org. Chem.*, 1999, **64**, 3012–3018; (c) S. J. Gharpure, A. M. Sathiyarayanan and P. Jonnalagadda, *Tetrahedron Lett.*, 2008, **49**, 2974–2978; (d) M. M. Toteva, M. Moran, T. L. Amyes and J. P. Richard, *J. Am. Chem. Soc.*, 2003, **125**, 8814–8819.
 - 15 (a) E. E. Weinert, R. Dondi, S. Colloredo-Melz, K. N. Frankenfield, C. H. Mitchell, M. Freccero and S. E. Rokita, *J. Am. Chem. Soc.*, 2006, **128**, 11940–11947; (b) R. W. Van de Water and T. R. R. Pettus, *Tetrahedron*, 2002, **58**, 5367–5405; (c) W.-J. Bai, J. G. David, Z.-G. Feng, M. G. Weaver, K.-L. Wu and R. R. Pettus, *Acc. Chem. Res.*, 2014, **47**, 3655–3664.
 - 16 M. M. Toteva and J. P. Richard, *Adv. Phys. Org. Chem.*, 2011, **45**, 39–91.
 - 17 G. Tsilomelekis, M. J. Orella, Z. Lin, Z. Cheng, W. Zheng, V. Nikolakis and D. G. Vlachos, *Green Chem.*, 2016, **18**, 1983–1993.
 - 18 The low yield of ether **9** after distillation is the result of a thermal fragmentation to the *ortho*-quinone methide followed by polymerization to undefined products. See also: (a) S. B. Cavith, H. R. Sarrafzadeh and P. D. Gardner, *J. Org. Chem.*, 1962, **27**, 1211–1216.